Chapter 22

Biophysical Methods to Analyze Direct G-Protein Regulation of Neuronal Voltage-Gated Calcium Channels

Norbert Weiss and Michel De Waard

Abstract

Neuronal voltage-gated calcium channels play an essential role for calcium entry into presynaptic endings responsible for the release of neurotransmitters. In turn, and in order to fine tune synaptic activity, numerous neurotransmitters exert a potent negative feedback over the calcium signal provided by G-protein-coupled receptors that can be recognized by characteristic biophysical modifications of the calcium current. There are two main biophysical approaches to analyze direct G-protein regulation of voltage-gated calcium channels: the so-called double-pulse method, which is indirectly assessed by the gain of current produced by a depolarizing prepulse potential, and the "subtraction" method that allows the analysis of G-protein regulation from the ionic currents induced by regular depolarizing pulses. The later method separates the ionic currents due to nonregulated channels from the ion currents that result from a progressive departure of G-proteins from regulated channels, thereby providing valuable information on the OFF kinetics of G-protein regulation. In this chapter, we introduce these "double pulses" and "subtraction" procedures for use primarily with single cells and also discuss the limitations inherent to these two approaches.

Key words Calciumchannel, Ca_v2 channel, G-protein-coupled receptor, G-proteins, Gβγ-dimer, Prepulse facilitation, Biophysical method

1 Introduction

Presynaptic voltage-gated calcium channels (VGCCs), primarily $Ca_v2.1$ and $Ca_v2.2$ channels, represent two of the most important players in the initiation of the Ca^{2+} signal by converting electrical impulses into intracellular Ca^{2+} elevations responsible for the release of neurotransmitters [6]. In turn, these channels are strongly regulated by a negative feedback mechanism provided by the activation of G-protein-coupled receptors (GPCRs) (for review, see [8, 36]). To date, up to 20 GPCRs have been described to modulate VGCCs (Table 1).

Direct inhibition of the Ca^{2+} channels occurs through the direct binding of G-protein βγ-dimer onto various structural molecular determinants of the Ca_v2-subunit [36]. At the whole

Rafael Luján and Francisco Ciruela (eds.), *Receptor and Ion Channel Detection in the Brain: Methods and Protocols*, Neuromethods, vol. 110, DOI 10.1007/978-1-4939-3064-7_22, © Springer Science+Business Media New York 2016

Table 1
Neurotransmitter- and receptor-mediated G-protein modulation of Ca_v2 channels

Neurotransmitter	Receptor	Ca_v channel	Tissue/species	Reference
Ach	M4	$Ca_v2.2$	SCG/rat	Bernheim et al. [2]
	M2	$Ca_v2.1$ & $Ca_v2.2$	SCG/mouse	Shapiro et al. [39]
Adenosine	A1	$Ca_v2.2$	Ciliary ganglion/chicken	Yawo and Chuhma [50]
		$Ca_v2.2$	DRG/chicken	Kasai and Aosaki [29]
		$Ca_v2.1$ & $Ca_v2.2$	Cerebellum/rat	Dittman and Regehr [10]
		$Ca_v2.2$ & $Ca_v2.3$	Hippocampus (CA3 → CA1)/rat	Wu and Saggau [47]
ATP/ADP	P2Y	$Ca_v2.2$	SCG/rat	Brown et al. [5], Filippov et al. [16]
Dopamine	D2	HVA	DRG/chicken	Marchetti et al. [32]
Endocannabinoids	CB1	$Ca_v2.1$	SCG/rat	Garcia et al. [18]
		$Ca_v2.1$, $Ca_v2.2$ & $Ca_v2.3$	Cerebellum	Brown and Russell [4]
GABA	GABA B	$Ca_v2.1$ & $Ca_v2.2$	DRG/rat	Dolphin and Scott [12]
			DRG/chicken	Deisz and Lux [9], Grassi and Lux [22]
			Cerebellum/rat	Dittman and Regehr [10]
		$Ca_v2.2$ & $Ca_v2.3$	Hippocampus (CA3 → CA1)/ guinea pig	Wu and Saggau [48]
		$Ca_v2.2$	SCG/rat	Filippov et al. [17]
Galanin	GalR1	$Ca_v2.2$	Hypothalamus/rat	Simen et al. [40]
Glutamate	mGluR1	$Ca_v2.2$	SCG/rat	Kammermeier and Ikeda [27]
LHRH	LHRH-R	$Ca_v2.2$	SCG/bullfrog	Elmslie et al. [15] Boland and Bean [3], Kuo and Bean [30]
Noradrenaline	α2-adrénergique	$Ca_v2.2$	SCG/bullfrog	Bean [1]
		$Ca_v2.2$	SCG/rat	Garcia et al. [19]
		Non-L	NG108-15	Docherty and McFadzean [11], McFadzean and Docherty [33]

NPY	Y2	Non-L $Ca_v2.2$	SCG/rat SCG/rat	Plummer et al. [35] Toth et al. [43]
Opioids – enkephalins	μ	$Ca_v2.2$	NG108-15	Kasai [28]
Opioids – dynorphins	κ	Non-L	DRG/rat	Bean [1]
Serotonin	5HT-1A	Non-L	Spinal neuron/lamprey	Hill et al. [23]
Somatostatin	SS-R	$Ca_v2.2$	DRG/rat	Ikeda and Schofield [26]
			SCG/rat	Ikeda and Schofield [25]
Substance P	NK1	$Ca_v2.2$	SCG/rat	Shapiro and Hille [38]
VIP	VIP-R	$Ca_v2.2$	SCG/rat	Zhu and Ikeda [52]

SCG superior cervical ganglion, *DRG* dorsal root ganglion

cell level, this regulation is recognized by various phenotypical modifications of the Ca^{2+} current, including a decrease of the inward current amplitude [3, 49], and in some cases a depolarizing shift of the voltage-dependence curve of current activation [1], and a slowing of activation [32] and inactivation kinetics [51]. In addition, short highly depolarizing voltage step, usually applied around +100 mV before the current eliciting pulse ("double-pulse" protocol), is sufficient to reverse, at least partially, most of the landmarks of G-protein inhibition. This protocol produces a so-called prepulse facilitation [13, 24, 37]. While the inhibition of the Ca^{2+} current has been attributed to the direct binding of G-protein βγ-dimer to the Ca_v2-subunit (referred as "ON" landmark for the onset of the inhibition), all the other landmarks including the slowing of current kinetics and prepulse facilitation can be described as variable time-dependent dissociation of Gβγ-dimer from the channel (referred as "OFF" landmarks for the arrest of the inhibition) and consequent recovery from G-protein inhibition [14, 41, 44]. Hence, proper attribution and precise quantitative evaluation of "ON" and "OFF" landmark parameters are necessary to assess the sensitiveness of a given calcium channel/GPCR complex and most importantly provide essential insight into the dynamic regulation of presynaptic calcium channels by G-proteins and GPCRs.

In this chapter, we provide a step-by-step illustration of the two main analytical methods that can be used to extract and describe the main parameters of "ON" and "OFF" G-protein landmarks. It is assumed that the reader already masters specific cell culture preparations and basic single cell patch-clamp recordings.

2 Methods

2.1 Biophysical Analysis of G-Protein Regulation by the "Double-Pulse" Method

The electrophysiological protocol classically used in the "double-pulse" method is shown in Fig. 1a. Initially introduced by Scott and Dolphin [37] and then widely adopted [13, 24], the method consists of comparing the peak current amplitude elicited by a given test pulse before (P1) and after (P2) application of a depolarizing prepulse of variable voltages and durations, both in control and G-protein-activated conditions. An example of current recordings is shown in Fig. 1b for $Ca_v2.2/\beta_3$ channels expressed in *Xenopus oocytes* in response to a 500 ms long test pulse elicited at 10 mV and a prepulse at 70 mV of variable durations. Notably, in control condition, a significant extent of current inactivation is produced by application of depolarizing prepulses as evidenced by a net decline of the peak current amplitude. In contrast, under G-protein activation, prepulse applications induce a current facilitation as evidenced by net-increased peak current amplitudes that

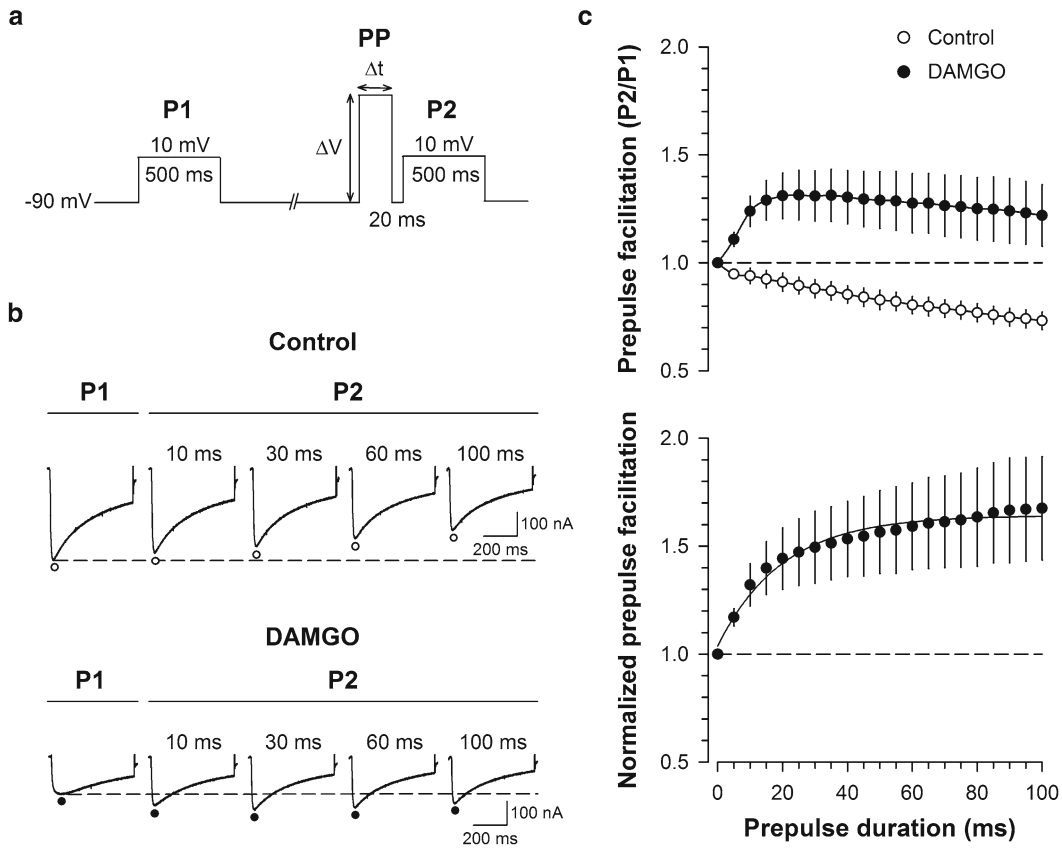

Fig. 1 Analysis of G-protein regulation by the "double-pulse" method. (**a**) Experimental protocol to measure prepulse-induced facilitation using the "double-pulse" method. P1 and P2, eliciting current pulses; *PP* prepulse. (**b**) Representative current traces recorded before and after G-protein activation by DAMGO, elicited by 500 ms P1 at 10 mV and 500 ms P2 at 10 mV following PP at 70 mV of variable durations. (**c**) Peak current amplitude ratio (P2/P1) for control (*open circles*) and DAMGO (*filled circles*) conditions (*top panel*). Normalized prepulse facilitation ($P2/P1_{DAMGO}$)/($P2/P1_{Control}$) to eliminate the prepulse-induced inactivation component resulting to the net prepulse facilitation kinetic. Fitting the result by a single exponential provides the time constant τ and maximal extent of prepulse facilitation (current recovery) (*bottom panel*) (Reproduced from Weiss and De Waard [45])

usually progressively decline with longer depolarizing prepulses. Under those conditions, elicited P2 currents are affected by a gain of current resulting from the dissociation of G-proteins from the channel (recovery from inhibition) and a loss of current due to channel inactivation induced by depolarizing prepulses. For short duration prepulses, the gain of current is predominant, whereas the tendency is inverted by increasing prepulse duration, at time points where G-protein dissociation saturates but channel inactivation increases. The control condition contains only the prepulse-induced inactivation component, whereas both the facilitation component and the inactivation component are present under

G-protein activation. Figure 1c illustrates the average behavior of normalized peak currents (P2/P1) plotted as a function of prepulse duration for both control and G-protein-activated conditions for a prepulse potential of 70 mV. In order to eliminate the inactivation component and isolate the net facilitation component under G-protein activation condition, the evolution of P2/P1 ratio observed under G-protein activation is normalized with regard to the evolution of P2/P1 ratio measured in control condition. The resulting result can then be best fitted by a single exponential function, providing the time constant of G-protein dissociation from the channel (t) and the maximal extent of current facilitation (current recovery). While τ provides important information about the kinetics of G-protein regulation, the extent of current facilitation assed by the "double-pulse" method indirectly gives access to the maximal amplitude of current inhibition that the activation of G-protein produced.

Note 1 Extracting parameters of G-protein regulation using the "double-pulse" method implies that control and G-protein-inhibited channels inactivate at the same rate and with a same extent. It also implies that the voltage dependence of this inactivation is not altered by G-protein inhibition. If this condition is not fulfilled, then the normalization procedure is flawed by approximation. So far, little information is available about the inactivation properties of the inhibited channel, but evidence points to the fact that G-protein-inhibited channels inactivate slower than control channels [15].

2.2 Biophysical Analysis of G-Protein Regulation by the "Subtraction" Method

In contrast to the "double-pulse" method, the "subtraction" method avoids the use of depolarizing prepulses and is not affected by possible alteration in channel inactivation kinetics induced by G-protein binding. This method extracts parameters of G-protein regulation from ionic currents elicited by regular depolarizing pulses by separating the ionic currents due to nonregulated channels from the ionic currents that result from the progressive unbinding of G-proteins from the regulated channel (current recovery). A step-by-step illustration of this method is illustrated in Fig. 2 using a representative example of a $Ca_v2.2/\beta_3$ channel expressed in *Xenopus oocytes* inhibited by application of the μ-opioid receptor agonist DAMGO.

1. Control ($I_{Control}$) and DAMGO-inhibited (I_{DAMGO}) currents, recorded before and after μ-opioid receptor activation, respectively, were triggered by a test pulse at 10 mV (Fig. 2a).
2. Subtracting I_{DAMGO} from $I_{Control}$ provides $I_{Inhibited}$, the amount of inhibited current upon G-protein activation (Fig. 2b, blue trace). The time course of the inhibited current is affected by both the recovery from G-protein inhibition that occurs

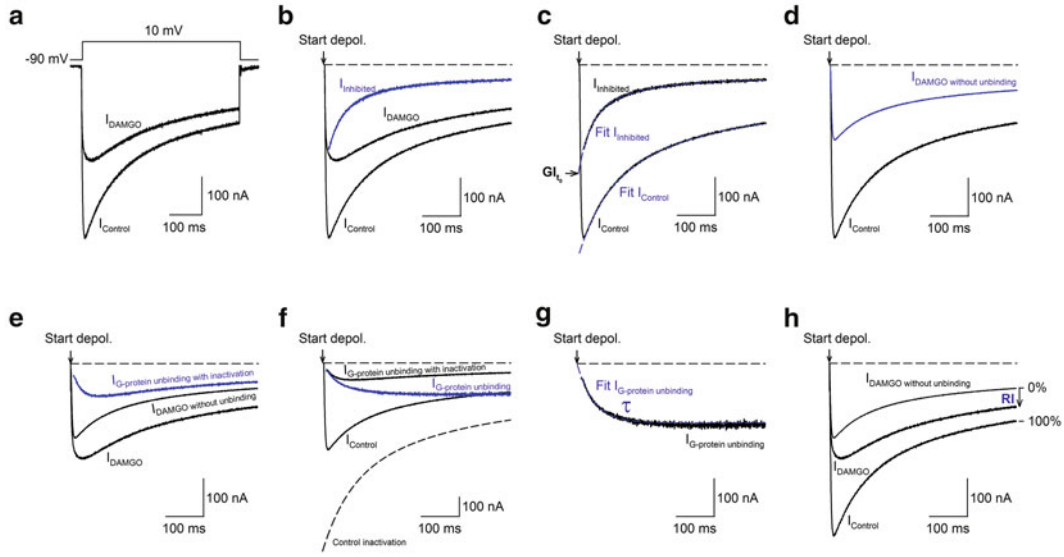

Fig. 2 Step-by-step illustration of the analysis of G-protein regulation by the "subtraction" method. (**a**) Representative current traces elicited at 10 mV for control ($I_{Control}$) and DAMGO (I_{DAMGO}) conditions. (**b**) Inhibited current ($I_{Inhibited}$, *blue trace*) under G-protein activation obtained by subtracting I_{DAMGO} from $I_{Control}$. The *dashed line* represents the zero current level and the *arrow* the start of the depolarization. (**c**) $I_{Control}$ and $I_{Inhibited}$ were extrapolated to $t = 0$ ms (start of the depolarization) by fitting traces (*blue dashed lines*) with a single and double exponential, respectively, in order to determine the maximal extent of G-protein inhibition (GIt_0). (**d**) Estimate of the fraction of control currents that is present in I_{DAMGO} ($I_{DAMGO\ without\ unbinding}$, *blue trace*) and that is due to a population of control channels. It is obtained by the following equation: $I_{Control} \times (1 - GIt_0)$. (**e**) The fraction of I_{DAMGO} current that recovers from G-protein inhibition (G-protein-inhibited channel population) is shown in *blue* ($I_{G\text{-}protein\ unbinding\ with\ inactivation}$) obtained by subtracting $I_{DAMGO\ without\ unbinding}$ from I_{DAMGO}. (**f**) The kinetics of G-protein dissociation ($I_{G\text{-}protein\ unbinding}$, *blue trace*) from G-protein-inhibited channels is obtained by dividing $I_{G\text{-}protein\ unbinding\ with\ inactivation}$ by the normalized control inactivation component (*dashed line* obtain by fitting $I_{Control}$ with a single exponential). (**g**) Fit of $I_{G\text{-}protein\ unbinding}$ (*dashed blue line*) by a single exponential decrease provides the time constant τ of G-protein dissociation from the channel. (**h**) Measure of the percentage of recovery from G-protein inhibition (RI) at the end of 500 ms pulse at 10 mV by $RI = (I_{DAMGO} - I_{DAMGO\ without\ unbinding})/(I_{Control} - I_{DAMGO\ without\ unbinding}) \times 100$ (Reproduced from Weiss and De Waard [45])

during the current eliciting pulse (conversion of G-protein-inhibited channels toward non-inhibited channels) and by the voltage-dependent inactivation of the channel that occurs during the eliciting pulse.

Note 2 One assumption is made that G-protein-bound channels do not undergo openings. It is worth to mention that ion-conducting openings of presumably G-protein-bound channels were initially proposed [7, 31], which could potentially affect the kinetics of $I_{Inihibited}$. However, openings of G-protein-bound channels remain difficult to assess directly and would require further investigation.

3. At the start of the eliciting pulse ($t = 0$ ms), there has been no recovery from G-protein inhibition, no opening from G-protein-bound channels, and inactivation has not taken place yet. Hence, in order to estimate the maximal extent of current inhibition produced by G-protein activation, I_{Control} and $I_{\text{Inhibited}}$ traces are extrapolated to $t = 0$ ms with a single and double exponential function, respectively (Fig. 2c, fits in blue). Fitting $I_{\text{Inhibited}}$ to $t = 0$ ms provides the first parameter of G-protein regulation termed GIt_0 for G-protein-induced current inhibition at the start of the depolarization and represents the maximal extent of current inhibition before any recovery process takes place ($GIt_0 = I_{\text{Inhibited}}\ t_0 / I_{\text{Control}}\ t_0 \times 100$ when expressed as percentage).
4. Applying this percentage of G-protein inhibition to I_{Control} results in $I_{\text{DAMGO without unbinding}}$, the theoretical current that would result from G-protein inhibition if the dissociation of G-proteins from the channel during the eliciting pulse did not occur at all (Fig. 2d, blue trace).
5. Subtracting $I_{\text{DAMGO without unbinding}}$ from I_{DAMGO} provides $I_{\text{G-protein unbinding with inactivation}}$ (Fig. 2e, blue trace). This current contains both the gain of current due to G-protein dissociation from the inhibited channels (recovery from inhibition) and inactivation of the gained current.

Note 3 The kinetics of the $I_{\text{G-protein unbinding with inactivation}}$ current are apparent since the gain of current is affected by inactivation, whereas inactivation is itself altered by the gain of current. Since the gained current results from the conversion of G-protein-inhibited channels toward non-inhibited channels, the real inactivation kinetics should be similar to the one of the non-inhibited channels. The amplitude of $I_{\text{G-protein unbinding with inactivation}}$ current will also depend on what extent inactivation of the channel may undergo during the depolarization when still in the G-protein-inhibited state. However, this inactivation will be significantly less than with a high depolarizing prepulse as the one that is applied in the "double-pulse" method.

6. In order to extract the net G-protein dissociation component, $I_{\text{G-protein unbinding with inactivation}}$ is divided by a normalized curve that depicts the inactivation of non-inhibited channels obtained by fitting I_{Control} by a single exponential function (Fig. 2f, dashed line). The resulting current $I_{\text{G-protein unbinding}}$ (Fig. 2f, blue trace) reflects the net kinetics of G-protein dissociation from the channel and reaches a stable plateau where no G-protein dissociation occurs anymore.
7. The kinetic τ of G-protein dissociation from the channel is obtained by fitting $I_{\text{G-protein unbinding}}$ by a decreasing single exponential function (Fig. 2g, blue dashed line). This time constant

represents the second essential parameter of G-protein regulation of voltage-gated calcium channels.

8. Finally, in order to get an estimate of the maximal fraction of G-protein-inhibited channels that recover from inhibition during the eliciting pulse, the percentage of current that had recovered from inhibition (RI) is measured such that: $RI = 100 \times (I_{DAMGO} - I_{DAMGO\ without\ unbinding}) / (I_{Control} - I_{DAMGO\ without\ unbinding})$ at a time point where $I_{G\text{-}protein\ unbinding}$ reaches a plateau. RI represents the third critical parameter that describes the calcium channel regulation by G-proteins.

3 Concluding Remarks

The biophysical analysis of direct G-protein regulation of voltage-gated calcium channels has been largely performed using the "double-pulse" method. This technique is easy to apply in both primary neurons in culture and heterologous expression systems including various mammalian cell lines and *Xenopus oocytes* and has been widely recognized and accepted. However, this approach makes the postulate that nonregulated and G-protein-inhibited channels inactivate with the same kinetics. Currently, because of technical difficulties to experimentally investigate this feature, there are no clear data in the literature supporting this assumption. In contrast, it is likely that G-protein bound channels inactivate at a slower rate than nonregulated channels, potentially introducing a significant bias to this procedure. This likelihood stems from the fact that Gβγ-dimers bind predominantly on one channel determinant that has been involved in the control of inactivation [42]. In contrast, the "subtraction" method does not require that G-protein-bound channels inactivate with the same kinetics than nonregulated channels. Moreover, this method does not require the application of a depolarizing prepulse that is usually applied along with an interpulse that provides an incentive for G-protein reassociation with the channel, therefore underestimating the real extent of G-protein dissociation. The "subtraction" analysis is exclusively based on current traces elicited at regular membrane voltages, before and after G-protein activation. Most importantly, this method allows the analysis of G-protein regulation at physiological membrane potential, providing a better understanding of the physiological dynamics of the regulation. It uncovers the importance of the offset of G-protein regulation in physiological processes rather than exclusively putting the emphasis on the onset of G-protein inhibition. This is a particularly important aspect of G-protein regulation knowing that neuronal networks undergo a significant extent of tonic G-protein activation. On the other hand, an inherent limitation of this approach is that it is limited to a range

of membrane potentials where ionic currents can be effectively measured. Although this method has been developed and validated on heterologous expressed channels, it is likely that it can also be suitable for analyzing G-protein regulation of voltage-gated calcium channels in native neuronal environment.

In summary, both of the described methods are not model independent and are both affected by their intrinsic assumptions and/or limitations. However, they provide similar qualitative information about the kinetics of the G-protein regulation and are therefore extremely informative in terms of how G-protein-coupled receptors dynamically regulate voltage-gated calcium channel in health and diseased state. Indeed, mutations in the genes encoding VGCCs linked to neurological disorders including hemiplegic migraine type 1 have been shown to alter direct G-protein regulation of mutated channels [20, 21, 34, 46]. Hence, perfect analysis of G-protein regulation of mutated channels not only contributes to our understanding of the associated channelopathies but also represent important signaling information for potential new therapeutic strategies.

Acknowledgments

Research in NW's laboratory is supported by the Czech Science Foundation (grant 15-13556S), the Ministry of Education Youth and Sports (grant 7AMB15FR015), and the Institute of Organic Chemistry and Biochemistry.

References

1. Bean BP (1989) Neurotransmitter inhibition of neuronal calcium currents by changes in channel voltage dependence. Nature 340:153–156
2. Bernheim L, Beech DJ, Hille B (1991) A diffusible second messenger mediates one of the pathways coupling receptors to calcium channels in rat sympathetic neurons. Neuron 6: 859–867
3. Boland LM, Bean BP (1993) Modulation of N-type calcium channels in bullfrog sympathetic neurons by luteinizing hormone-releasing hormone: kinetics and voltage dependence. J Neurosci 13:516–533
4. Brown CH, Russell JA (2004) Cellular mechanisms underlying neuronal excitability during morphine withdrawal in physical dependence: lessons from the magnocellular oxytocin system. Stress 7:97–107
5. Brown DA, Filippov AK, Barnard EA (2000) Inhibition of potassium and calcium currents in neurones by molecularly-defined P2Y receptors. J Auton Nerv Syst 81:31–36
6. Catterall WA (2011) Voltage-gated calcium channels. Cold Spring Harb Perspect Biol 3:a003947
7. Colecraft HM, Patil PG, Yue DT (2000) Differential occurrence of reluctant openings in G-protein-inhibited N- and P/Q-type calcium channels. J Gen Physiol 115: 175–192
8. De Waard M, Hering J, Weiss N, Feltz A (2005) How do G proteins directly control neuronal Ca2+ channel function? Trends Pharmacol Sci 26:427–436
9. Deisz RA, Lux HD (1985) gamma-Aminobutyric acid-induced depression of calcium currents of chick sensory neurons. Neurosci Lett 56:205–210
10. Dittman JS, Regehr WG (1996) Contributions of calcium-dependent and calcium-independent mechanisms to presynaptic inhibition at a cerebellar synapse. J Neurosci 16:1623–1633
11. Docherty RJ, McFadzean I (1989) Noradrenaline-induced inhibition of voltage-sensitive

calcium currents in NG108-15 hybrid cells. Eur J Neurosci 1:132–140

12. Dolphin AC, Scott RH (1987) Calcium channel currents and their inhibition by (-)-baclofen in rat sensory neurones: modulation by guanine nucleotides. J Physiol 386:1–17
13. Doupnik CA, Pun RY (1994) G-protein activation mediates prepulse facilitation of Ca2+ channel currents in bovine chromaffin cells. J Membr Biol 140:47–56
14. Elmslie KS, Jones SW (1994) Concentration dependence of neurotransmitter effects on calcium current kinetics in frog sympathetic neurones. J Physiol 481:35–46
15. Elmslie KS, Zhou W, Jones SW (1990) LHRH and GTP-gamma-S modify calcium current activation in bullfrog sympathetic neurons. Neuron 5:75–80
16. Filippov AK, Brown DA, Barnard EA (2000) The P2Y(1) receptor closes the N-type Ca(2+) channel in neurones, with both adenosine triphosphates and diphosphates as potent agonists. Br J Pharmacol 129:1063–1066
17. Filippov AK, Couve A, Pangalos MN, Walsh FS, Brown DA, Moss SJ (2000) Heteromeric assembly of GABA(B)R1 and GABA(B)R2 receptor subunits inhibits Ca(2+) current in sympathetic neurons. J Neurosci 20:2867–2874
18. Garcia DE, Brown S, Hille B, Mackie K (1998) Protein kinase C disrupts cannabinoid actions by phosphorylation of the CB1 cannabinoid receptor. J Neurosci 18:2834–2841
19. Garcia DE, Li B, Garcia-Ferreiro RE, Hernandez-Ochoa EO, Yan K, Gautam N, Catterall WA, Mackie K, Hille B (1998) G-protein beta-subunit specificity in the fast membrane-delimited inhibition of Ca2+ channels. J Neurosci 18:9163–9170
20. Garza-Lopez E, Gonzalez-Ramirez R, Gandini MA, Sandoval A, Felix R (2013) The familial hemiplegic migraine type 1 mutation K1336E affects direct G protein-mediated regulation of neuronal P/Q-type Ca2+ channels. Cephalalgia 33:398–407
21. Garza-Lopez E, Sandoval A, Gonzalez-Ramirez R, Gandini MA, Van den Maagdenberg A, De Waard M, Felix R (2012) Familial hemiplegic migraine type 1 mutations W1684R and V1696I alter G protein-mediated regulation of Ca(V)2.1 voltage-gated calcium channels. Biochim Biophys Acta 1822:1238–1246
22. Grassi F, Lux HD (1989) Voltage-dependent GABA-induced modulation of calcium currents in chick sensory neurons. Neurosci Lett 105:113–119
23. Hill RH, Svensson E, Dewael Y, Grillner S (2003) 5-HT inhibits N-type but not L-type Ca(2+) channels via 5-HT1A receptors in lamprey spinal neurons. Eur J Neurosci 18:2919–2924
24. Ikeda SR (1991) Double-pulse calcium channel current facilitation in adult rat sympathetic neurones. J Physiol 439:181–214
25. Ikeda SR, Schofield GG (1989) Somatostatin blocks a calcium current in rat sympathetic ganglion neurones. J Physiol 409:221–240
26. Ikeda SR, Schofield GG (1989) Somatostatin cyclic octapeptide analogs which preferentially bind to SOMa receptors block a calcium current in rat superior cervical ganglion neurons. Neurosci Lett 96:283–288
27. Kammermeier PJ, Ikeda SR (1999) Expression of RGS2 alters the coupling of metabotropic glutamate receptor 1a to M-type K+ and N-type Ca2+ channels. Neuron 22:819–829
28. Kasai H (1992) Voltage- and time-dependent inhibition of neuronal calcium channels by a GTP-binding protein in a mammalian cell line. J Physiol 448:189–209
29. Kasai H, Aosaki T (1989) Modulation of Ca-channel current by an adenosine analog mediated by a GTP-binding protein in chick sensory neurons. Pflugers Arch 414:145–149
30. Kuo CC, Bean BP (1993) G-protein modulation of ion permeation through N-type calcium channels. Nature 365:258–262
31. Lee HK, Elmslie KS (2000) Reluctant gating of single N-type calcium channels during neurotransmitter-induced inhibition in bullfrog sympathetic neurons. J Neurosci 20:3115–3128
32. Marchetti C, Carbone E, Lux HD (1986) Effects of dopamine and noradrenaline on Ca channels of cultured sensory and sympathetic neurons of chick. Pflugers Arch 406:104–111
33. McFadzean I, Docherty RJ (1989) Noradrenaline- and enkephalin-induced inhibition of voltage-sensitive calcium currents in NG108-15 hybrid cells. Eur J Neurosci 1:141–147
34. Melliti K, Grabner M, Seabrook GR (2003) The familial hemiplegic migraine mutation R192Q reduces G-protein-mediated inhibition of P/Q-type (Ca(V)2.1) calcium channels expressed in human embryonic kidney cells. J Physiol 546:337–347
35. Plummer MR, Rittenhouse A, Kanevsky M, Hess P (1991) Neurotransmitter modulation of calcium channels in rat sympathetic neurons. J Neurosci 11:2339–2348
36. Proft J, Weiss N (2015) G-protein regulation of neuronal calcium channels: back to the future. Mol Pharmacol 87:890–906
37. Scott RH, Dolphin AC (1990) Voltage-dependent modulation of rat sensory neurone calcium channel currents by G protein activation: effect of a dihydropyridine antagonist. Br J Pharmacol 99:629–630

38. Shapiro MS, Hille B (1993) Substance P and somatostatin inhibit calcium channels in rat sympathetic neurons via different G protein pathways. Neuron 10:11–20
39. Shapiro MS, Loose MD, Hamilton SE, Nathanson NM, Gomeza J, Wess J, Hille B (1999) Assignment of muscarinic receptor subtypes mediating G-protein modulation of Ca(2+) channels by using knockout mice. Proc Natl Acad Sci U S A 96:10899–10904
40. Simen AA, Lee CC, Simen BB, Bindokas VP, Miller RJ (2001) The C terminus of the Ca channel alpha1B subunit mediates selective inhibition by G-protein-coupled receptors. J Neurosci 21:7587–7597
41. Stephens GJ, Brice NL, Berrow NS, Dolphin AC (1998) Facilitation of rabbit alpha1B calcium channels: involvement of endogenous Gbetagamma subunits. J Physiol 509:15–27
42. Stotz SC, Hamid J, Spaetgens RL, Jarvis SE, Zamponi GW (2000) Fast inactivation of voltage-dependent calcium channels. A hinged-lid mechanism? J Biol Chem 275:24575–24582
43. Toth PT, Bindokas VP, Bleakman D, Colmers WF, Miller RJ (1993) Mechanism of presynaptic inhibition by neuropeptide Y at sympathetic nerve terminals. Nature 364:635–639
44. Weiss N, Arnoult C, Feltz A, De Waard M (2006) Contribution of the kinetics of G protein dissociation to the characteristic modifications of N-type calcium channel activity. Neurosci Res 56:332–343
45. Weiss N, De Waard M (2007) Introducing an alternative biophysical method to analyze direct G protein regulation of voltage-dependent calcium channels. J Neurosci Methods 160:26–36
46. Weiss N, Sandoval A, Felix R, Van den Maagdenberg A, De Waard M (2008) The S218L familial hemiplegic migraine mutation promotes deinhibition of Ca(v)2.1 calcium channels during direct G-protein regulation. Pflugers Arch 457:315–326
47. Wu LG, Saggau P (1994) Adenosine inhibits evoked synaptic transmission primarily by reducing presynaptic calcium influx in area CA1 of hippocampus. Neuron 12:1139–1148
48. Wu LG, Saggau P (1995) GABAB receptor-mediated presynaptic inhibition in guinea-pig hippocampus is caused by reduction of presynaptic Ca2+ influx. J Physiol 485:649–657
49. Wu LG, Saggau P (1997) Presynaptic inhibition of elicited neurotransmitter release. Trends Neurosci 20:204–212
50. Yawo H, Chuhma N (1993) Preferential inhibition of omega-conotoxin-sensitive presynaptic Ca2+ channels by adenosine autoreceptors. Nature 365:256–258
51. Zamponi GW (2001) Determinants of G protein inhibition of presynaptic calcium channels. Cell Biochem Biophys 34:79–94
52. Zhu Y, Ikeda SR (1994) VIP inhibits N-type Ca2+ channels of sympathetic neurons via a pertussis toxin-insensitive but cholera toxin-sensitive pathway. Neuron 13:657–669